Measuring method of loss for optical waveguides by use of a rectangular glass probe

By

Ikuo AWAI*, Hidetoshi ONODERA**,
Masamtisu NAKAJIMA** and Jun-ichi IKENOUE***

(Received July 13, 1984)

Abstract

The use of a glass-plate probe of rectangular shape is proposed for the measurement of transmission loss in thin-film optical waveguides. The light-collecting window is of a thin rectanglar shape perpendicular to the light streak, while the conventional fiber probe has a very small circular face. This transversely elongated form results in a great improvement of the mechanical tolerance for the probe movement in the vertical as well as the transverse direction. Theoretical investigation is also presented in reasonable agreement with the experiments.

1. Introduction

There have been two non-destructive methods to measure the transmission loss of optical planar waveguides[1]. One of them is known as the sliding prism method. When a certain mode is supported on a slab waveguide, the mode power is coupled out with a prism that is slided along the light streak. Plotting of the output power vs. prism distance gives an exponential decay constant of the mode. Though this technique has the advantage that it is applicable even to a low-loss waveguide, it has the following disadvantages: (1) It is not easy to keep the output efficiency constant as the prism slides, because of the mechanical fluctuation in the course of the movement. (2) Frequent attachment and removal of the prism to and from the waveguide damages the waveguide as well as the prism itself.

Another method of loss measurement may be called the scattered-light detecting method. Detection can be made either by a probe with a photo diode or by a camera (including a TV camera). Being a non-contacting detection, it is free from the disadvantages (2) above. This method, however, has the following weak point. Detection with a probe, though much simpler and less expensive than that with a camera, has a disadvantage similar to (1) of the sliding prism method.

* Department of Electronics. Present adress: Uniden Satellite Technology Inc., Tokyo.
** Department of Electronics.
*** Department of Electronics. Present adress: Fukuyama University, Fukuyama.

In this paper, we have taken up this probe method and attempted to overcome the defects. Our proposal is to use a glass-plate probe instead of a fiber probe. A circular cylindrical glass probe will also be examined for comparison.

2. Probe configuration and experimental set-up

Since fiber probes which have been commonly used are of a small cross-section, it is difficult for the prove to follow along the light streak with a constant distance spaced between them both vertically and horizontally. The output from the fiber probe often deviates from exponential decay because of the fluctuation of the probe movement. In order to avoid the effect of the horizontal fluctuation, a probe scanning measurement has been analyzed and the maximum outputs have been plotted to obtain an exponential decay. But this technique still suffers from the vertical fluctuation of the probe, and hence the improvement of accuray is limited in spite of the complication of the measurement system.

We have then adopted a glass rod of a circular cross section, considering that it forms a waveguide without cladding and that it has a wide light-collecting window which may bring about better mechanical tolerance compared with a thin fiber probe. The thicker a probe is, the more stable becomes the output with respect to the vertical or horizontal fluctuation of the probe. But we cannot make it too thick since the waveguide to be measured has finite length. When a probe is thicker, the range l of a constant coupling coefficient is smaller, as is shown in Fig.

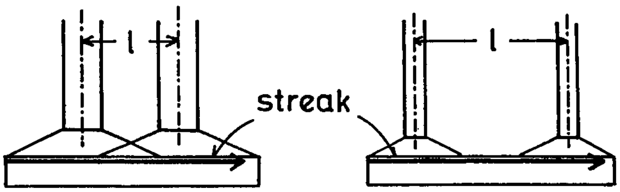

Fig. 1. Dependence of the range l of correct measurement upon the thickness of the probe.

1. Thus, we should limit the longitudinal dimension of the probe with the transverse dimension kept wide enough, which results in a rectangular probe arranged as shown in Fig. 2. In this way, it is expected that the probe has both the relaxed tolerance of movement and the wide range of constant coupling efficiency.

A Si photo cell is used as a detector attached to the other end of the probe, as is illustrated in Fig. 3. It is wide enough to catch all the signals which come out from the probe. The low sensitivity of a Si photo cell is compensated by the use of a locked-in amplifier. Any other type of glass may also be feasible for the probe, but only if it is transparent and has all the surfaces polished.

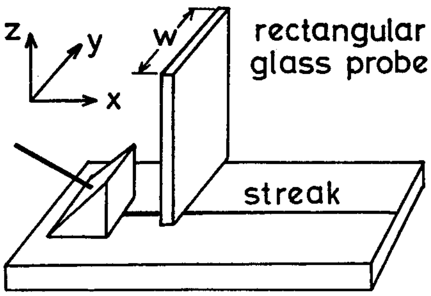

Fig. 2. Arrangement of the rectangular glass probe on planar waveguide.

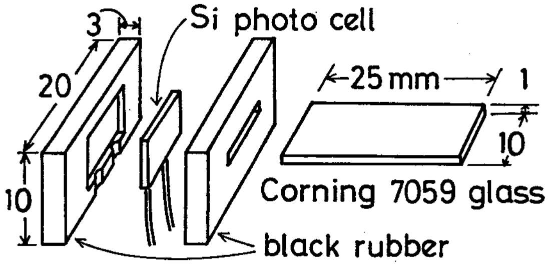

Fig. 3. The structure of the detecting part.

Figure 4 is a block diagram of the measurement system. The probe is mounted on an *XYZ* mechanical stage. Since the stray light degrades the S/N ratio, a black absorber is painted on all the surfaces of the waveguide substrate, except the upper waveguiding part. An automatic measurement will be easily attained if the output of the locked-in amplifier is put in a log amplifier, and the logarithmic output is plotted agianst the longitudinal movement of the probe using an *XY* recorder. The output linearity of the Si photo cell was good enough for the present use, as long as the streak was not too bright.

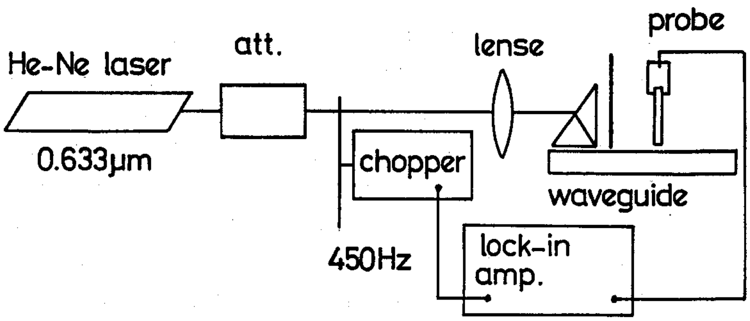

Fig. 4. Schematic of the loss measurement system.

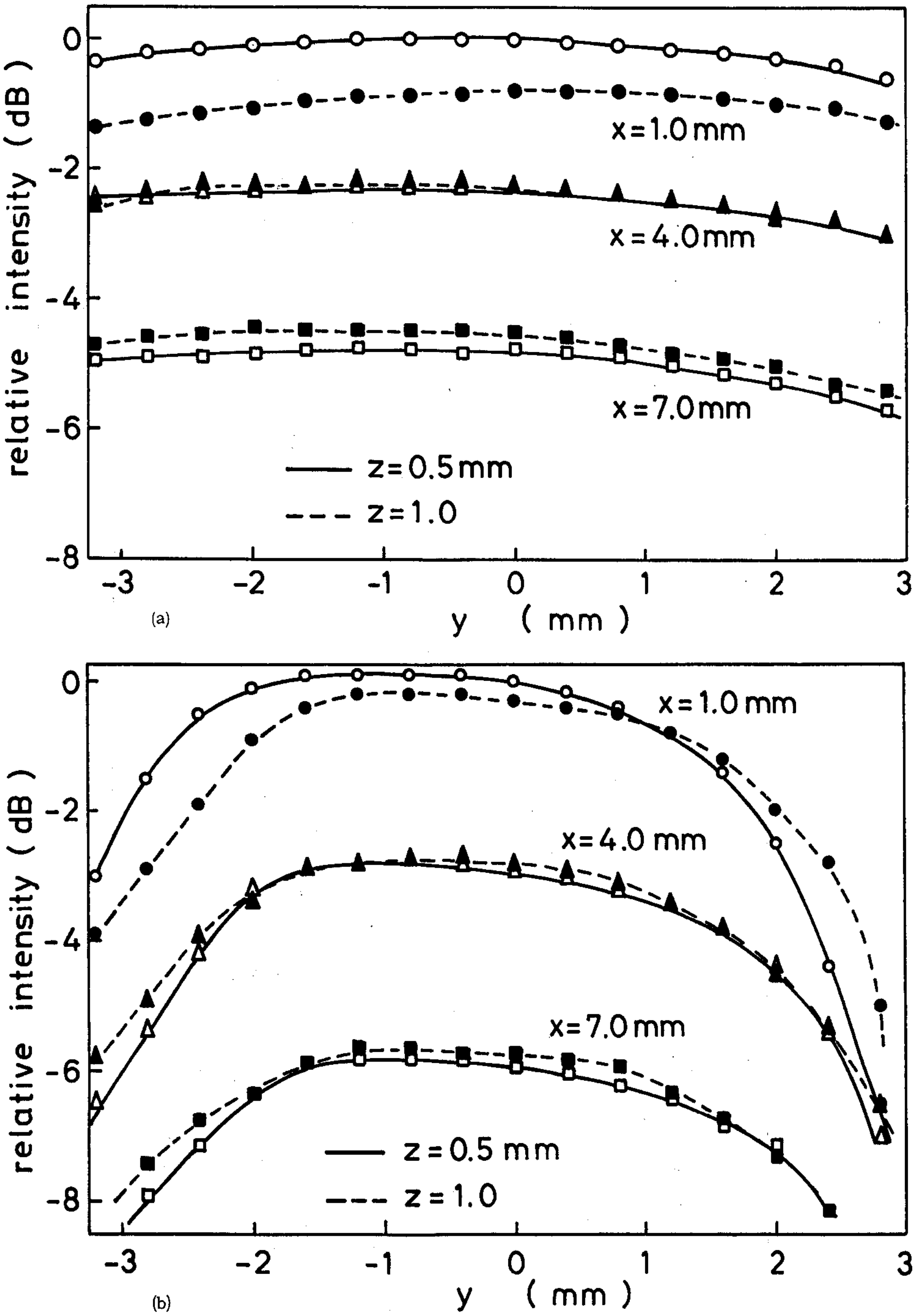

Fig. 5. Output intensity of a rectangular probe as a function of transverse deviation (probe thickness: 1 mm, waveguide loss 10 dB/cm).
(a) Probe width : 10 mm (b) Probe width : 4 mm

3. Mechanical tolerance

(1) Transverse deviation

As the probe deviates from the light streak transversely (in the y-direction in Fig. 2), the collected light at the window of the probe will decrease monotonically. But it will be almost constant as far as the deviation is less than half the probe width. This expectation is demonstrated to be true in Fig. 5, by two experiments with rectangular probes of different widths. The flatness of the output is satisfactory even for the narrower probe, because the transverse probe deviation can easily be kept less than 1 mm. The waveguide loss is as high as 10 dB/cm in this example.

We have also made a comparative experiment using a circular cylindrical probe.

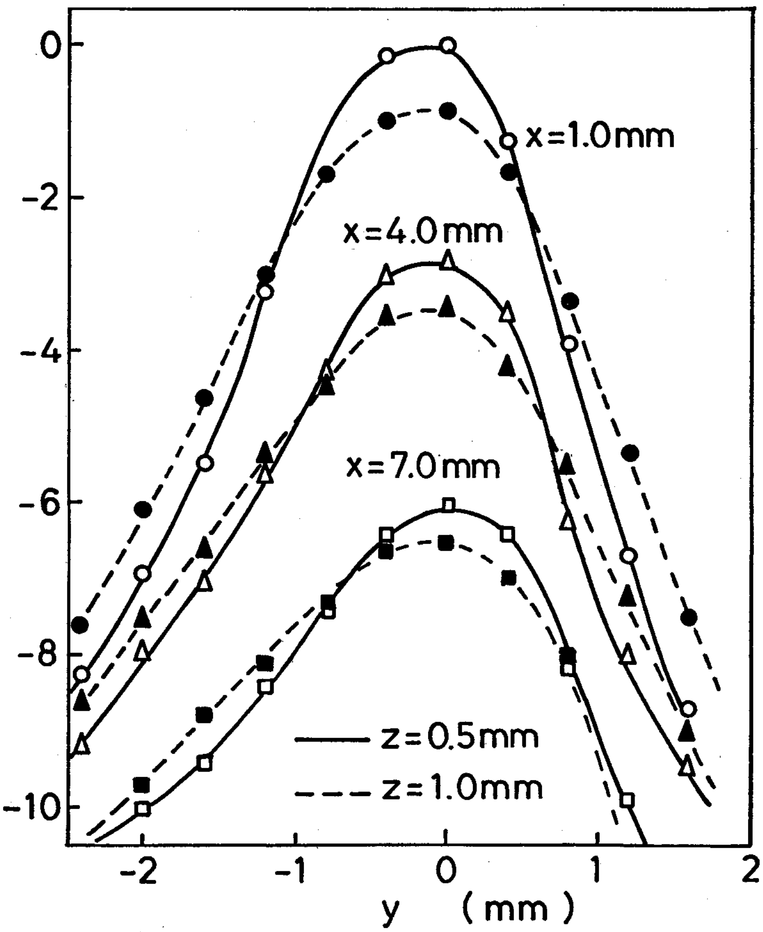

Fig. 6. Output intensity of a circular cylindrical probe as a function of transverse deviation (Probe diameter : 1.5 mm, waveguide loss : 10 dB/cm).

This probe resembles a conventional fiber probe in the shape of a cross-section, while it differs in that it is much thicker and has no cladding. In fact, the diameter of our probe is no less than 1.5 mm. Figure 6 tells us that a probe of a circular cross section is sensitive to the transverse deviation even if it is fairly thick. If it shifts transversely by 1 mm, the output decreases more than 3 dB.

(2) Vertical deviation

A detecting probe fluctuates also vertically (in the z-direction in Fig. 2) when one moves it along the light streak in order to measure the attenuation constant of waveguides. The output variation against the probe height is plotted in Fig. 7. The probe widths are 4 and 10 mm, the thickness being kept at 1 mm. Though it may seem strange that the output increases with height for larger distances from the input prism, this characteristic can be explained as follows.

Let us consider the limiting case where the waveguide is lossless, and hence

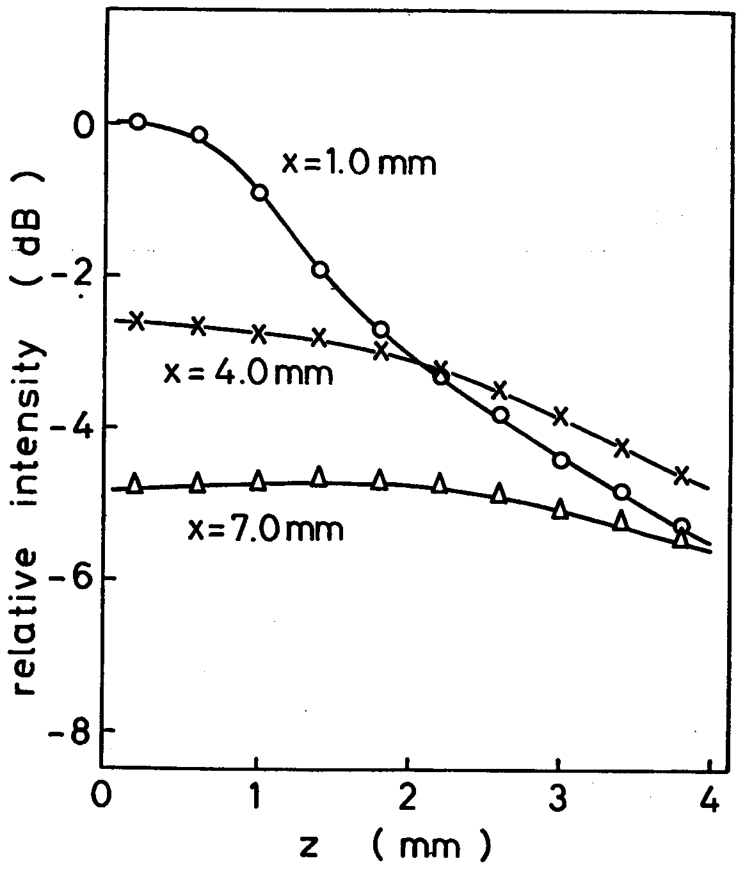

(a)

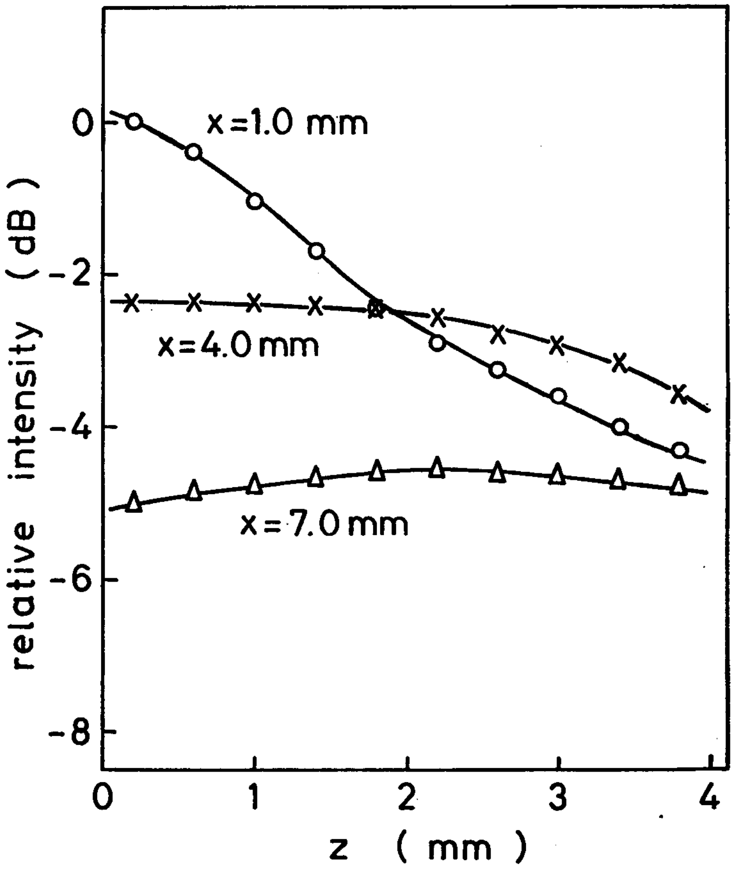

(b)

Fig. 7. Output intensity of a rectangular probe as a function of vertical deviation (Probe thickness : 1 mm, waveguide loss : 10 dB/cm).
(a) Probe width : 10 mm (b) Probe width : 4 mm

the intensity of the light streak is constant. If the probe were infinitely wide in the y-direction, the incident flux into the probe would not change with the probe height. This means a wide rectangular probe will be very insensitive to the vertical fluctuation if the waveguide loss is small. On the contrary, if the waveguide loss is very large, as in the case of Fig. 7, the streak is much stronger at smaller x. Therefore, the probe collects more flux when it goes up, because the stronger light from the source (more to the left) enters the probe with a smaller incident angle as shown in Fig. 8.

Figure 9 illustrates the vertical tolerance of a circular cylindrical probe. This is a well-behaved example for a probe of a circular cross-section, since it is much

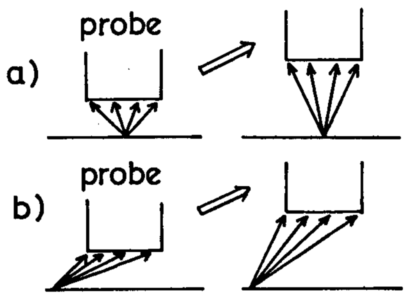

Fig. 8. The reason why the output of a wide rectangular probe increases with the probe height when the waveguide loss is very large.

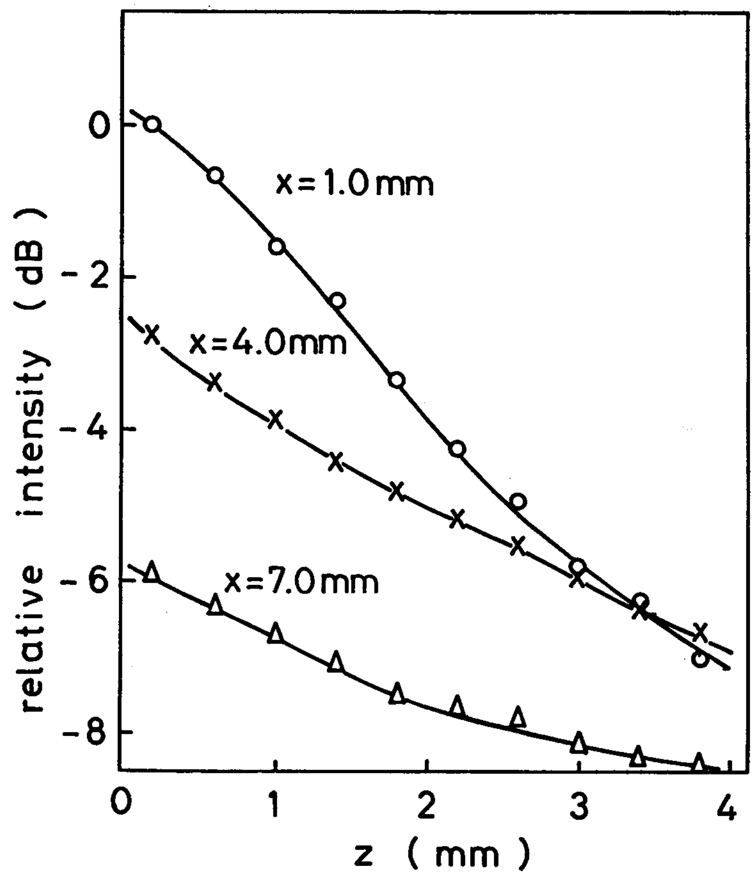

Fig. 9. Output intensity of a circular cylindrical probe as a function of vertical deviation (Probe diameter : 1.5 mm, waveguide loss 10 dB/cm).

thicker than a usual fiber probe.

4. Loss measurement

After examining the mechanical tolerance of the system in Fig. 4, we have constructed an automatic measurement system, mentioned in Sec. 2. The input to the x-axis of the recorder is provided by a potentiometer connected to the rotary shaft of the optical XYZ-stage. The lowest TE mode was excited by a rutile prism. Attenuation constants are estimated from the slope of the straight (hopefully) lines drawn by an XY-recorder.

We will show some of the results in Fig. 10. Figure 10(a) is for the Nb_2O_5-Corning 7059 glass structure. The Nb_2O_5 amorphous film was fabricated by an rf magnetron sputtering apparatus in the Ar ; 80%-O_2 ; 20% atmosphere with the substrate water-cooled. The refractive indices of the film and the substrate were 2.25 and 1.53 respectively, and the film thickness was 0.3μm. Since the film was so thin, the attenuation constant was calculated to be as high as 6.9 dB/cm. The light streak was of a very high intensity and uniform, indicating that the attenuation comes mainly from the surface scattering. This type of waveguide is one of the easiest for applying the scattered-light detecting method.

The second example is shown in Fig. 10 (b), which is for the Nb_2O_5-$LiTaO_3$ structure. The Nb_2O_5 film was fabricated in the same way as the former example. Though this waveguide had a smaller loss of 3.0 dB/cm, the streak was more non-uniform, indicating many randomly-located scattering points. It corresponds to type

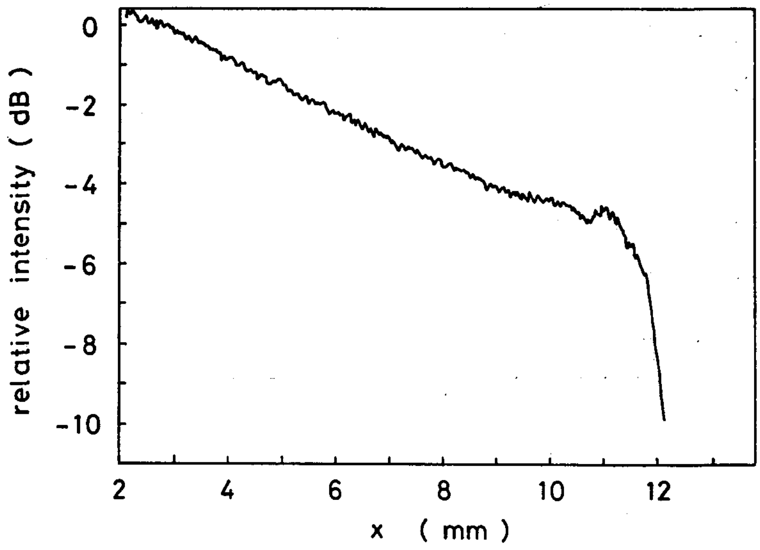

(a)

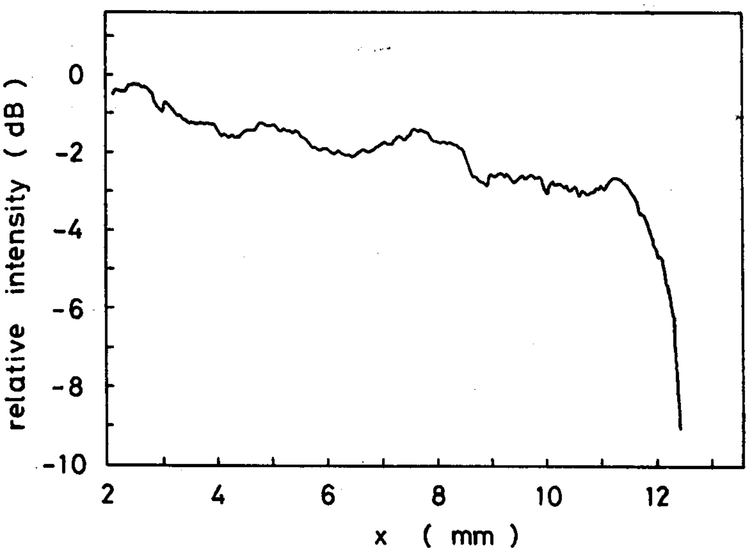

(b)

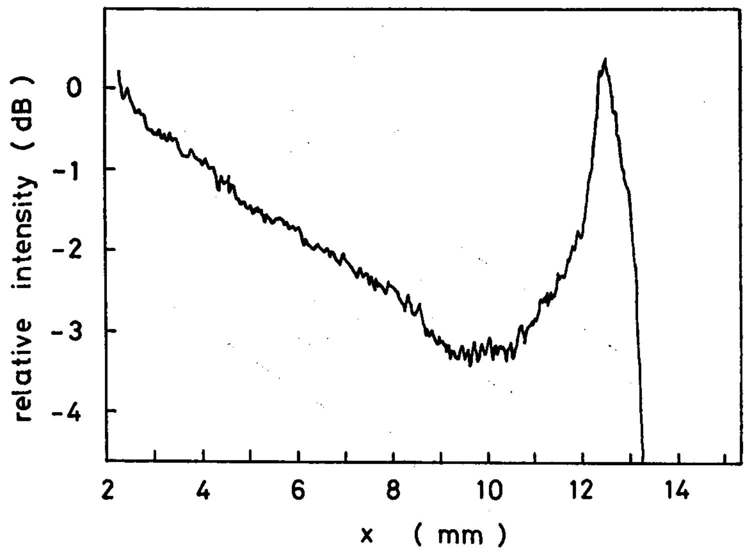

(c)

Fig. 10. Three examples of automatic loss measurement.
(a) Nb_2O_5-Corning 7059 waveguide.
(b) Nb_2O_5-$LiTaO_3$ waveguide.
(c) Nb diffused $LiTaO_3$ waveguide.

(b) of the three categories of Gottlieb's paper[2].

The third waveguide was created by Nb-indiffusion into the z-cut $LiTaO_3$ substrate. Niobium of 0.061μm thickness was deposited by an electron beam evaporator and diffused for 3 hours in the air. A high peak has appeared on the right in Fig. 10 (c), because the edge of the waveguide was not painted black in this case. Though the intensity of the guided light was weak, the attenuation constant was fairly large, which means that the loss mechanism was mainly absorption in the guide, or that most of the scattered light went downward[3] and was absorbed by the black paint at the bottom.

5. Theoretical formulation

Since this probing system has a simple structure, it seems that the output characteristic could be easily calculated. There are, however, many obstacles which hinder the formulation of the problem. These are illustrated in Fig. 11 with the numbers in which order they are explained below.

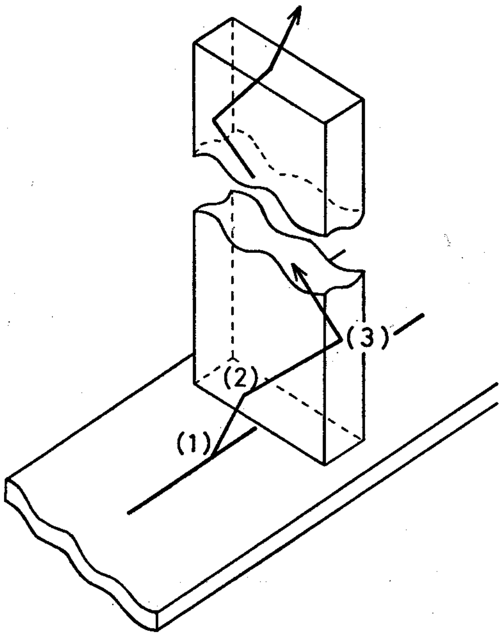

Fig. 11. Three diffiiculties in formulating the output of a rectangular probe.

First, it is not known how much light reaches the probe, because the directivity (radiation pattern) of the scattered light from a streak differs from waveguide to waveguide[2)4)5)].

Secondly, the transmission coefficient in the probe is different according to the polarization of incident light, and it depends on what mode is excited.

Thirdly, the light caught in the probe goes upward, repeating total reflection at the side walls of the probe. Since the polarizations change at each reflection, the ratio of the p and s polarizations of the output light varies with the reflection angle at each wall. This results in a change of the photo cell output.

A formulation which takes into account the above-mentioned points is not impossible, but unnecessarily complicated. Thus, we will make the following simplifications.

(1) The radiation pattern from the light streak is a cosine function of the polar angle which takes a maximum value at a certain direction.

(2) The polarization of the scattered light from the light streak is equally distributed in p and s directions (no polarization).

(3) All the energy entering into the probe is detected by the photo cell.

We have examined experimentally the response of the detecting system composed of the probe and the photo cell, so as to confirm the validity of assumption (3). The incident angle dependence is shown in Fig. 12, indicating a close agreement with the theory. The theoretical curves are obtained by the product of $\cos\psi$ and the transmission coefficient T_p or T_s at the air glass interface, where ψ denotes the incident angle at the probe end face, and

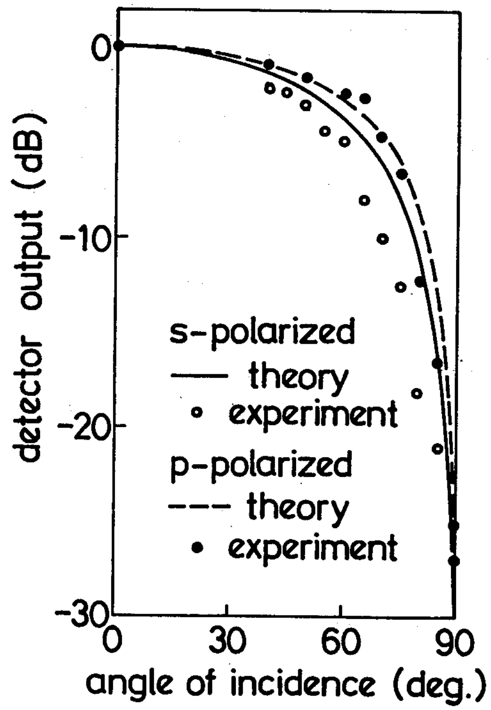

Fig. 12. Detector output as a function of incident angle of collimated beam.

$$T_p=1-\frac{\tan^2(\psi-\psi')}{\tan^2(\psi+\psi')}$$
$$T_s=1-\frac{\sin^2(\psi-\psi')}{\sin^2(\psi+\psi')} \quad (1)$$
$$\psi'=\sin^{-1}\left(\frac{1}{n_g}\sin\psi\right)$$

Figure 13 shows the coordinate system and the probe configuration. We draw a line ♯1 which passes through the point (l, 0, 0) on the streak, makes an angle θ with the z-axis and lies in the x-z plane (incident plane). The direction cosine of

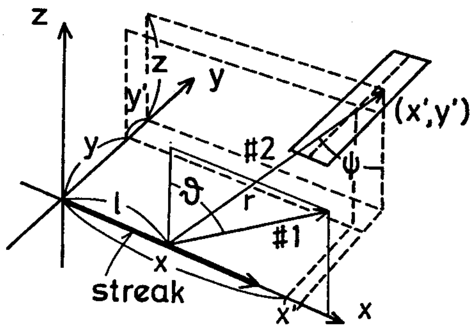

Fig. 13. Coordinate system for calculating the flux incident into the end face of a probe.

line ♯1 is ($\sin\theta$, 0, $\cos\theta$). We introduce another coordinate system (x', y') for the infinitesimal element dx', dy' on the probe end face. The line between this element and point (l, 0, 0) is denoted as ♯2, the direction cosine (α, β, γ) being given by

$$\alpha=\frac{x+x'-l}{r},\quad \beta=\frac{y+y'}{r},\quad \gamma=\frac{z}{r}, \quad (2)$$

where

$$r=\sqrt{(x+x'-l)^2+(y+y')^2+z^2}. \quad (3)$$

Here we introduce χ for the angle between lines ♯1 and ♯2, so that we obtain the relation

$$\cos\chi=\alpha\sin\theta+\gamma\cos\theta. \quad (4)$$

Substituting eqs. (2) and (3) into eq. (4) yields

$$\cos\chi=\frac{(x+x'-l)\sin\theta+z\cos\theta}{\sqrt{(x+x'-l)^2+(y+y')^2+z^2}}. \quad (5)$$

The flux incident to the element $dx'dy'$ from the source Idl at (l, 0, 0) is written as

$$dP'=Idl\cdot\frac{dx'dy'\cos\psi}{r^2}\cdot\cos\chi, \quad (6)$$

where the second term on the right-hand side is the solid angle spanning the ele-

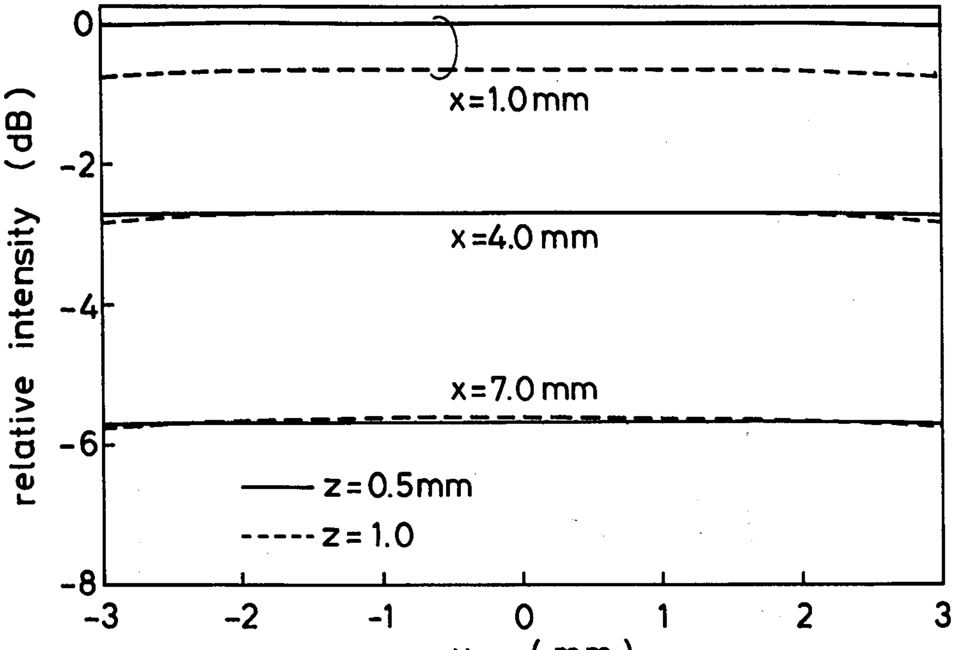

(a)

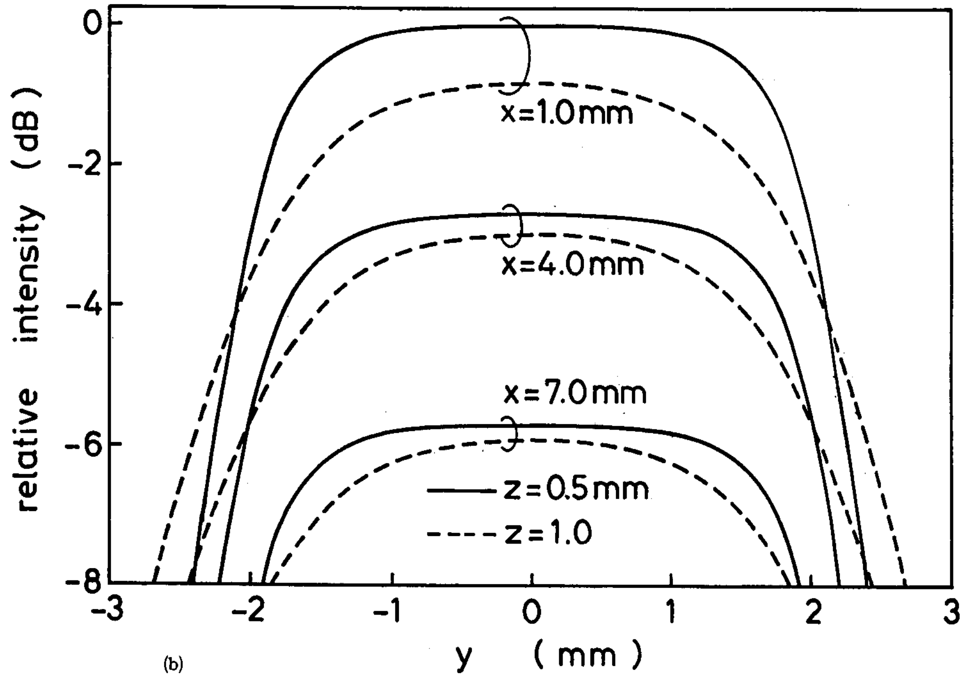

(b)

Fig. 14. Theoretical output intensity of a rectangular probe as a function of transverse deviation (Probe thickness : 1 mm, waveguide loss 10 dB/cm).
(a) Probe width : 10 mm (b) Probe width : 4 mm

ment $dx'dy'$ from the source at $(l, 0, 0)$. The angle ψ between line ♯2 and the direction of the probe end face obviously satisfies the relation

$$\cos\psi=\frac{z}{r}=\frac{z}{\sqrt{(x+x'-l)^2+(y+y')^2+z^2}} \tag{7}$$

Now, we can integrate eq. (6) to get the total flux

$$P=\int_{-\frac{w}{2}}^{\frac{w}{2}}\int_{-\frac{t}{2}}^{\frac{t}{2}}\int_{0}^{\infty}\frac{I_0e^{-\alpha l}\cos\psi\cos\chi T}{r^2}dldx'dy', \tag{8}$$

where α denotes the attenuation constant of the waveguides, w and t are the width and thickness of the rectangular probe respectively, and the averaged transmission coefficient T is given by

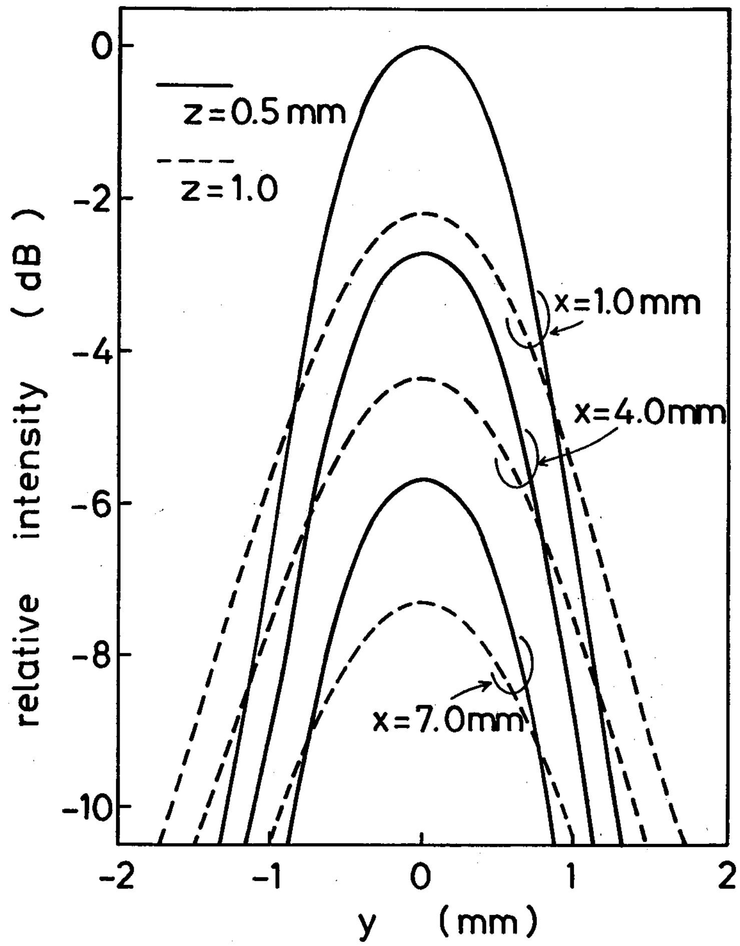

Fig. 15. Theoretical output intensity of a circular cylindrical probe as a function of transverse deviation (Probe diameter : 1.5 mm, waveguide loss : 10 dB/cm).

$$T=\frac{T_p+{}_sT}{2}. \tag{9}$$

6. Computed results and discussions

The triple integral of eq. (8) was executed numerically by a FACOM-M 382 computer. The calculated mechanical tolerance is elucidated in Figs. 14 and 16. The parameters were chosen to be the same as Figs. 5 and 7 respectively. The angle of directivity θ was taken to be 0 degree since it gave the best fitting between the experimental and theoretical curves. They are qualitatively in good agreement. In fact, examining the z-dependence of the output of Fig. 16, we notice that the output increases with small z when the probe width w is large, while it decreases with z when w is small. This feature agrees with the experimental result, as shown in Fig. 7.

Figures 15 and 17 are for a circular cylindrical probe, corresponding to Figs. 6 and 8. The experimental and theoretical results also agree well in this case.

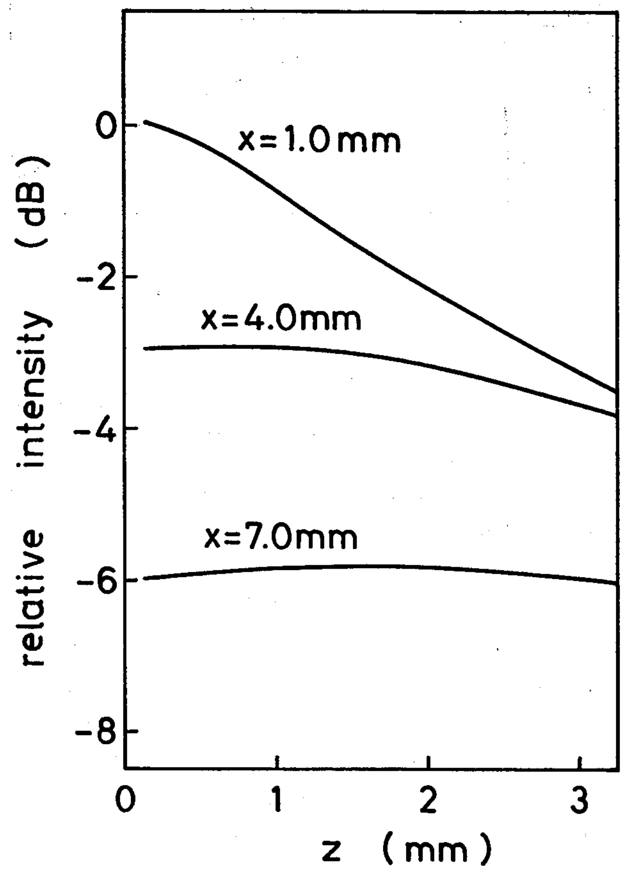

(a)

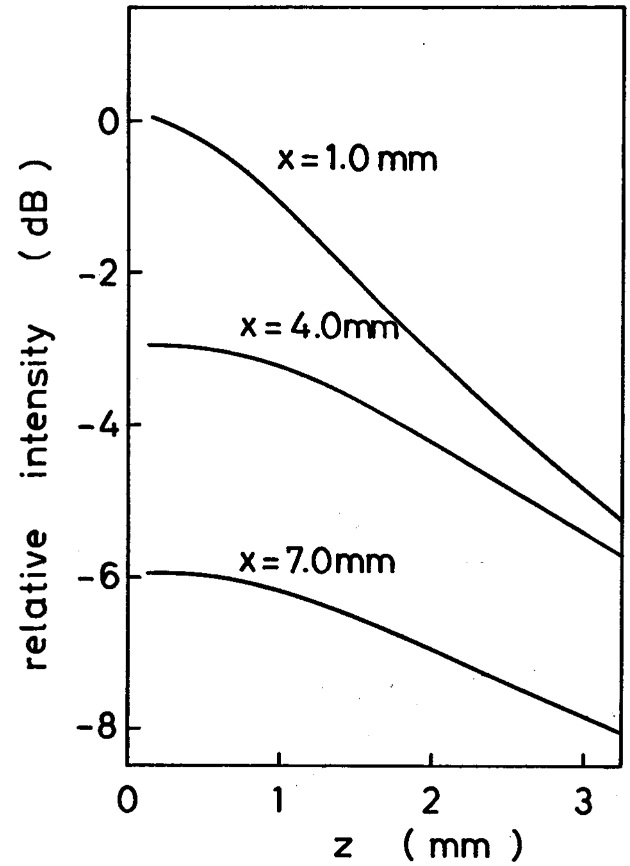

(b)

Fig. 16. Theoretical output intensity of a rectangular probe as a function of vertical deviation (Probe thickness: 1 mm, waveguide loss: 10 dB/cm). (a) Probe width: 10 mm (b) Probe width: 4 mm

It is concluded that a rectangular probe exhibits a much better characteristic than a circular cylindrical probe does.

7. Conclusion

We have taken up "the scattered light probing method" which has been extensively employed for planar-waveguide loss measurement. We proposed to use a rectangular glass probe instead of a conventional fiber glass one. Our probe means a conversion from a one-dimensional end face to a two-dimensional one, since the cross section of a fiber glass probe is like a point, whereas that of a rectangular probe is like a line. It resulted in a significant improvement of the mechanical tolerance of the probe movement as well as an increase of the detecting signal.

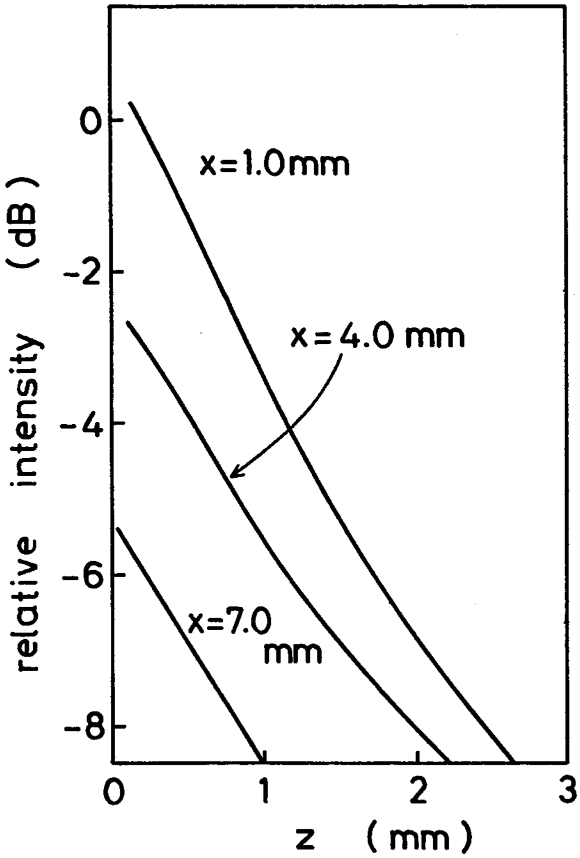

Fig. 17. Theoretical output intensity of a circular cylindrical probe as a function of vertical deviation (Probe diameter : 1.5 mm, waveguide loss 10 dB/cm).

These characteristics made it easier to automatize the measurement. Also, the time for measurement was reduced considerably.

References

1) J. E. Goell and R. D. Standley, "Sputtered Glass Waveguide for Integrated Optical Circuits", Bell Syst. Tech. J. Briefs, **48**, 3445 (1969).
2) M. Gottlieb, G. B. Brandt and J. J. Conroy, "Out-of-Plane Scattering in Optical Waveguides", IEEE Trans. Circuits Syst., **CAS-26**, 1029 (1979).
3) Y. Suematsu and K. Furuya, "Characteristic Modes and Scattering Loss of Asymmetric Slab Optical Waveguides", Electron. and Commun. in Japan, **56-C**, 277 (1973).
4) S. Miyanaga, M. Imai and T. Asakura, "Radiation Pattern of Light Scattering from the Core Region of Dielectric-Slab-Optical Waveguides", IEEE J. Quantam Electron., **QE-14**, 30 (1978).
5) Y. Suematsu, K. Furuya, M. Hakuta and K. Chiba, "Far Field Radiation Pattern Caused by Random Wall Distortion of Dielectric Waveguides and Determination of Correlation Length", Electron. and Commun. in Japan, **56-C**, 377 (1973).